

EDA: Explicit Text-Decoupling and Dense Alignment for 3D Visual and Language Learning

Yanmin Wu¹, Xinhua Cheng¹, Renrui Zhang^{2,4}, Zesen Cheng¹, Jian Zhang^{1,3*}

¹ School of Electronic and Computer Engineering, Peking University, China

² The Chinese University of Hong Kong, China

³ Peng Cheng Laboratory, China ⁴ Shanghai AI Laboratory, China

{wuyanmin, chengxinhua, cyanlaser}@stu.pku.edu.cn, zhangjian.sz@pku.edu.cn, zhangrenrui@pjlab.org.cn

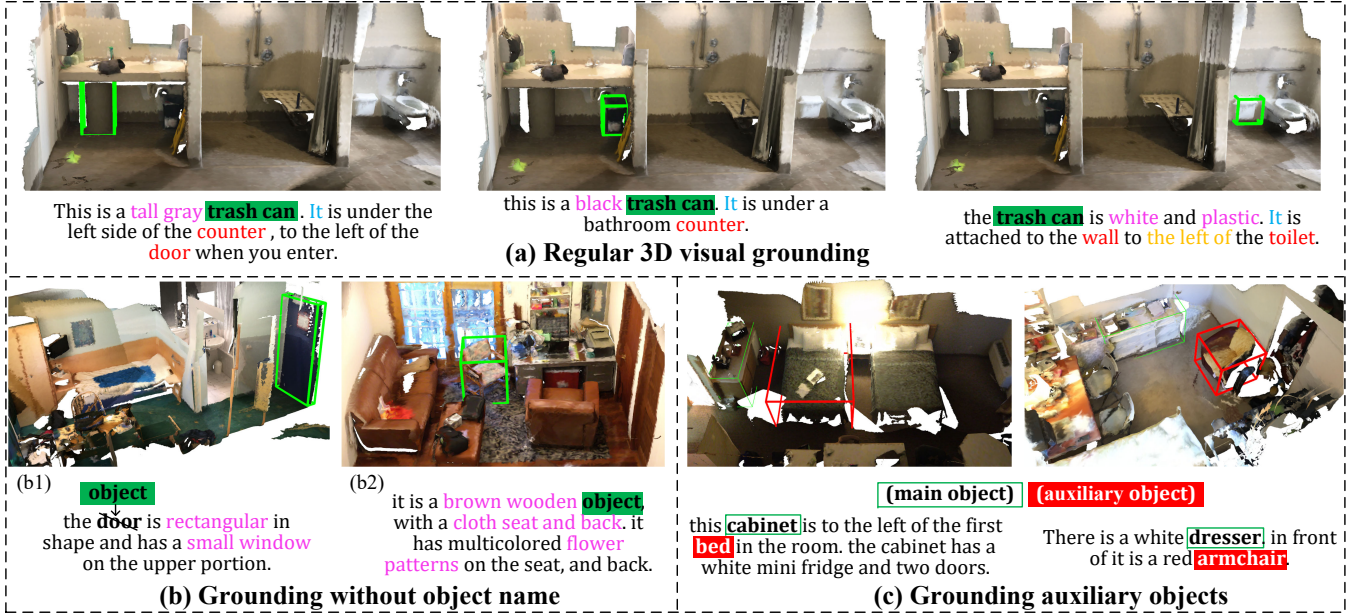


Figure 1: Text-decoupled, dense aligned 3D vision-language tasks. (a) Regular visual grounding: locating objects requires comprehensively considering multiple semantic cues such as appearance attributes, object names, and spatial relationships. (b) Grounding without object name: not mentioning object names, forcing the model to predict the target based on other attributes. (c) Grounding the auxiliary object: jointly find the main object and the auxiliary object referenced in the utterance.

Abstract

3D visual grounding aims to find the objects within point clouds mentioned by free-form natural language descriptions with rich semantic components. However, existing methods either extract the sentence-level features coupling all words, or focus more on object names, which would lose the word-level information or neglect other attributes. To alleviate this issue, we present **EDA** that **Explicitly Decouples** the textual attributes in a sentence and conducts **Dense Alignment** between such fine-grained language and point cloud objects. Specifically, we first propose a text decoupling module to produce textual features for every semantic component. Then, we design two losses to supervise the dense matching between two modalities: the textual position alignment and object semantic alignment. On top of that, we further introduce two new visual grounding tasks, locating objects without object names and locating auxiliary objects referenced in the descriptions, both of which can thoroughly evaluate the model's dense alignment capacity. Through experiments, we achieve

state-of-the-art performance on two widely-adopted visual grounding datasets, ScanRefer and SR3D/NR3D, and obtain absolute leadership on our two newly-proposed tasks. The code will be available at <https://github.com/yanmin-wu/EDA>.

1 Introduction

The multi-modal cues can highly benefit the environment perception of an agent, including 2D images, 3D point clouds, and language. Recently, **3D visual grounding** (3D VG) (Chen, Chang, and Nießner 2020), also known as object referencing (Achlioptas et al. 2020), has attracted much attention as an important 3D cross-modal task. Its objective is to find the target object in point cloud scenes by analyzing the corresponding descriptive language, which requires understanding both 3D visual and linguistic context.

Typically, the language descriptions involve words concerning appearance attributes, object categories, and spatial

relationships, as shown by different colors in Fig. 1, and the network requires integrating most of them to locate objects. Existing works have made great progress from the following perspectives: improving point cloud features extraction by sparse convolution (Yuan et al. 2021) or 2D images’ assistance (Yang et al. 2021); obtaining more discriminative object candidates through instance segmentation (Huang et al. 2021) or language modulation (Luo et al. 2022); modeling spatial relationships between entities via graph convolution (Feng et al. 2021) or Transformer (Cai et al. 2022). However, we observe two issues that still remain unexplored: **1)** In some cases, the target object is too much trivial for the network to find, or the interference candidates can be eliminated solely based on the object category (such as the “door” in Fig. 1(b1)). This might cause the model produce an inductive bias for such object category and weaken the learning of other attributes. Meanwhile, it is also common that the object name do not appear in the utterance (see Fig. 1(b2)). **2)** Some utterances might mention multiple objects (like the main and auxiliary objects in Fig. 1(c)), while the objective is to locate only the main object, leading to an imbalanced and ambiguous understanding of language descriptions. These insufficiencies of existing works stem from their characteristic of feature coupling and fusing implicitly. They input a sentence with different attribute words but output only one globally **coupled** text feature that is subsequently matched with the visual features of candidate objects. The coupled text features are ambiguous because some words may not describe the main object but the auxiliary object. Alternatively, using the cross-modal attention of Transformer (Vaswani et al. 2017; Dosovitskiy et al. 2021) to **implicitly** fuse local visual and text features. However, this may encourage the model to take shortcuts, such as focusing on object categories and ignoring other attributes, as previously discussed.

Instead, we propose a more intuitive decoupled and explicit strategy. First, we parse the input text to **decouple** different semantic components, including the main object word, pronoun, attributes, relations, and auxiliary object words. Then, performing **dense alignment** between vision and decoupled language achieves fine-grained feature matching, which avoids the inductive bias resulting from imbalanced learning of different textual components. As the final grounding result, we **explicitly** select the object with the highest similarity to the decoupled text components of the main object (instead of the entire text). Additionally, to explore the limits of VG and examine the comprehensiveness and fine-graininess of visual-language perception of the model, we suggest two challenging new tasks: **1) Grounding without object name (VG-w/o-N)**, where the name is replaced by “object” (see Fig. 1(b)), forcing the model to locate objects based on other attributes; **2) Grounding the auxiliary object (VG-AO)**, such as “bed” and “armchair” in Fig. 1(c), requires a complete understanding of the text content. Benefit from our decoupling operation, we can leverage the text component of the auxiliary object to match visual features. Besides, thanks to the supervision of our dense aligned losses, all text components are aligned with visual features rather than depending only on object names.

To sum up, the main contributions of this paper are as follows: **1)** We propose a text decoupling module to parse linguistic descriptions into multiple semantic components, followed by suggesting the well-designed dense aligned losses for supervising fine-grained visual-language feature fusion. **2)** Two novel tasks are proposed to comprehensively examine the model’s performance. **3)** We achieve state-of-the-art performance on two datasets on the regular VG task and absolute leadership on two new tasks.

2 Related Work

2.1 3D Vision and Language

3D vision and language are vital manners for humans to understand and perceive the environment, and they are also important research topics for the evolution of machines to be like humans. In 3D visual grounding, the speaker (like a human) describes an object in language. The listener (such a robot) needs to understand the language description and the 3D visual scene to grounding the target object. On the contrary, the 3D dense caption (Chen et al. 2021b,a; Yuan et al. 2022; Jiao et al. 2022; Wang et al. 2022) is analogous to an inverse process in which the input is a 3D scene, and the output is textual descriptions of each object. Moreover, language-modulated 3D detection or segmentation (Jain et al. 2022; Rozenberszki, Litany, and Dai 2022) enriches the diversity of queries and overcomes the limits of conventional fixed semantic labels. 3D vision and language have previously evolved independently. In recent years, as the trend of multimodality (Qi et al. 2020; Radford et al. 2021; Ramesh et al. 2022) has only begun, there are many open and practical topics worth exploring.

2.2 3D Visual Grounding

The majority of current mainstream techniques are two-stage, extracting visual and textual features independently, then performing multimodal feature fusion and predicting the referring result. Most use pre-trained language models (Devlin et al. 2018) or 3D object detectors (Qi et al. 2019) or segmenters (Jiang et al. 2020) for the first stage. Second-stage feature fusion is the primary concern. **1)** The most naïve solution is concatenating the two modal features and then considering it as a binary classification problem (Achlioptas et al. 2020; Kumar, Patro, and Nambodiri 2022), which provides limited performance. **2)** Taking advantage of the nature of Transformer’s attention mechanism that is naturally suitable for feature fusion, some works (He et al. 2021; Zhao et al. 2021) have achieved remarkable performance by doing self-attention and cross-attention to features. **3)** In contrast, other studies view feature fusion as a matching problem rather than a classification. (Yuan et al. 2021) and (Abdelreheem et al. 2022), supervised by the contrastive loss (He et al. 2020), compute the cosine similarity of visual features and textual features. Inspired by (Liu et al. 2020), (Feng et al. 2021) parses the text to generate a text scene graph, simultaneously builds a visual scene graph, and then performs graph node matching. **4)** Due to point clouds’ sparse, noisy nature and lacking detail, making it challenging to learn complete semantic information about objects,

some studies (Yang et al. 2021; Cai et al. 2022) use 2D images to aid visual-textual feature fusion, but at the cost of additional 2D-3D alignment and 2D feature extraction.

However, the two-stage method has a substantial detection bottleneck: objects overlooked in the first stage cannot be matched in the second. (Liu et al. 2021a) suggests fusing visual and linguistic features at the bottom level and producing text-related visual heatmaps. Similarly, (Luo et al. 2022) presents a single-stage approach that employs textual features to guide visual keypoint selection and progressively localizes objects. Beauty-DETR (Jain et al. 2022) is also a semi-single-stage fashion, but more importantly, it measures the similarity between each word and object, then selects the features of the word corresponding to the object’s name to match the candidate object. However, there are two limitations: 1) Since multiple object names may be mentioned in a sentence, the GT annotation is used to determine the target name, limiting its generalizability. Our text decoupling separates text components to avoid this restriction. 2) Only the **sparse alignment** of main object words to visual features is considered. Conversely, we align all decoupled textual semantic components with visual features, which we refer to **dense alignment**, significantly enhancing the discriminability of multimodal features.

3 Proposed Method

The framework is illustrated in Fig. 3. First, the input text description is decoupled into multiple semantic components, and its affiliated text positions and features are obtained (Sec. 3.1). Concurrently, the Transformer-based encoder extracts and modulates features from point clouds and text, then decodes the visual features of candidate objects (Sec. 3.2). Finally, the dense aligned losses are derived between the decoupled text features and the decoded visual features (Sec. 3.3). The grounding result is the object with visual features most similar to text features (Sec. 3.4).

3.1 Text Decoupling

The text features of the coupled fashion are ambiguous, where features from multiple objects and attributes are coupled, such as “a brown wooden chair next to the black table.” Among them, easy-to-learn features (such as the colour “brown”) may predominate, weakening other attributes (such as material “wooden”), and words of other objects (such as the “black table”) may cause interference. To produce more discriminative text features and fine-grained cross-modal feature fusion, we decouple text into different semantic components, each of which is independently aligned with visual features.

1) Text Component Decoupling Analyzing grammatical dependencies between words is a fundamental task in NLP. We first use the off-the-shelf tool (Schuster et al. 2015; Wu et al. 2019) to parse the language description grammatically to generate the grammatical dependency trees, as shown in Fig. 2. Each sentence contains only one ROOT node, and each remaining word has a corresponding parent node. Then according to the words’ part-of-speech and dependencies, we decouple the long text into five semantic components:

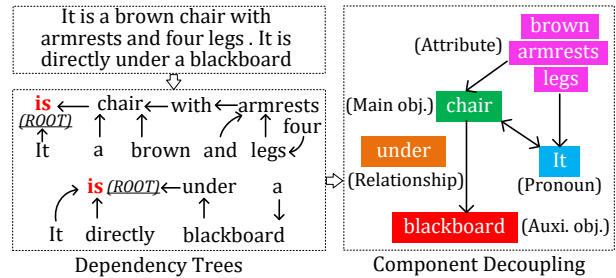


Figure 2: Text component decoupling.

Main object - the target object mentioned in the utterance; Auxiliary object - the one used to assist in locating the main object; Attributes - objects’ appearance, shape, etc.; Pronoun - the word instead of the main object; Relationship - the spatial relation between the main object and the auxiliary object. Note that attributes affiliated with pronouns are equivalent to attached with the main object, thus connecting two sentences in an utterance.

2) Text Position Decoupling After decoupling each text component (Fig. 3(a)), we generate the position label $L \in \mathbb{R}^{1 \times l}$ for the component’s associated word (Fig. 3(b)). Where $l=256$ is the maximum length of the text, each component’s word position is set to 1 and the rest to 0. The label will be used to supervise the classification of objects. The classification result, however, is not one of a fixed number of object categories but rather the position of the text with the closest semantic similarity.

3) Text Feature Decoupling In the backbone network of multimodal feature extraction, the feature of each word (token) is produced (Fig. 3(d)), and the text feature of the decoupled component can be derived by dot-multiplying it with the respective component position label, as shown in Fig. 3(c). The decoupled text features will be aligned separately with the visual features. Note that in the decoupled features, the semantics of the corresponding components predominate, but as a result of the Transformer’s attention mechanism, it also implicitly contains the global semantic information of the entire sentence.

3.2 Multimodal Feature Extraction

We employ Beauty-DETR’s encoder-decoder module for feature extraction and intermodulation of cross-modal features, as shown in Fig. 3(d)(e)(f). Essentially, our method is not restricted to the feature extraction backbone.

Input Modal Tokenization. The input text and 3D point clouds are encoded by the pre-trained RoBERTa (Liu et al. 2019) and pointnet++ (Qi et al. 2017) and produce text token $\mathcal{T} \in \mathbb{R}^{l \times d}$ and visual token $\mathcal{V} \in \mathbb{R}^{n \times d}$, respectively. Additionally, the GroupFree (Liu et al. 2021b) detector is used to detect 3D boxes and encoded as the box token $\mathcal{B} \in \mathbb{R}^{b \times d}$. Note that the box input is optional, the final predicted object of the network is from the visual token, and the box token is to assist in better regression of the target object.

Encoder-Decoder. Self-attention and cross-attention are performed in the encoder to update both visual and text fea-

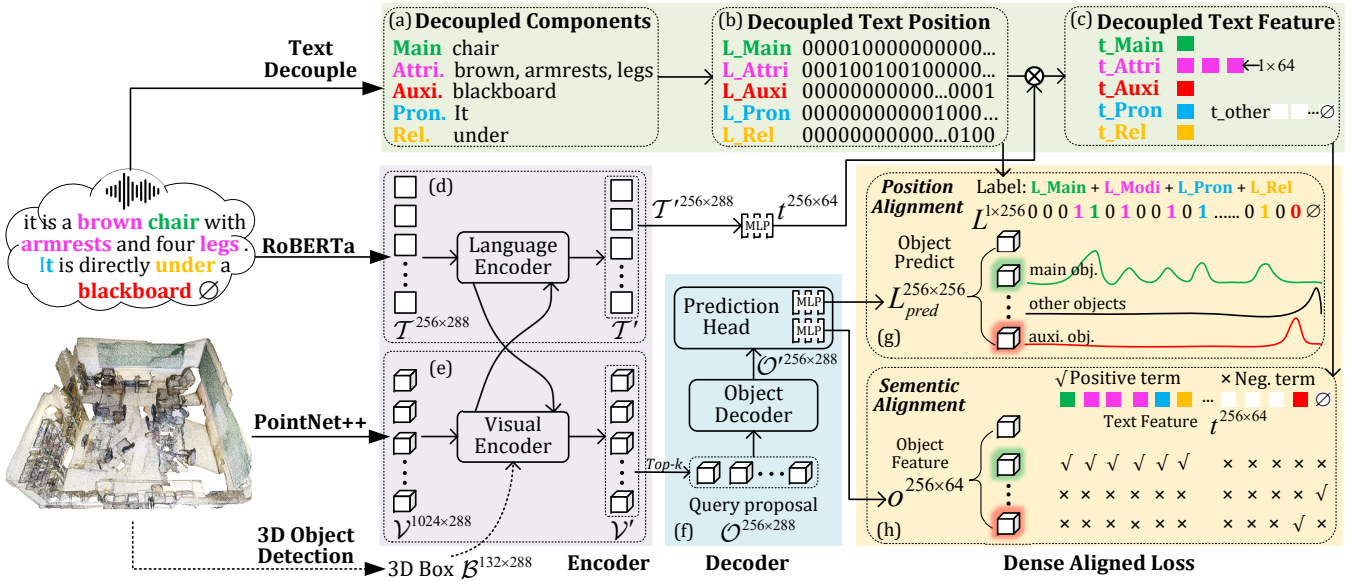


Figure 3: The system framework. (a-c): Decouple the input text into several components to acquire the position label and features of the decoupled text. (d-e): Transformer-based encoders for cross-modal vision-text feature extraction. (f): Decode candidate object features. (g-h): Visual-text feature dense alignment.

tures, obtaining cross-modal features $\mathcal{V}', \mathcal{T}'$ while keeping the dimensions. The top- k ($k=256$) visual features are selected, linearly projected as query proposal features $\mathcal{O} \in \mathbb{R}^{k \times d}$, and updated as \mathcal{O}' in the decoder.

Prediction Head. The proposal features $\mathcal{O}' \in \mathbb{R}^{k \times d}$ are fed into MLPs to predict the position labels $L_{pred} \in \mathbb{R}^{k \times l}$ of the corresponding text, which are then utilized to calculate the position alignment loss with L . In addition, the proposal features are linearly projected as $\mathcal{o} \in \mathbb{R}^{k \times 64}$ by other MLPs, producing the semantic alignment loss with the also linearly projected text feature $\mathbf{t} \in \mathbb{R}^{l \times 64}$.

3.3 Dense Aligned Loss

1) Dense Position Aligned Loss The objective of position alignment is to ensure that the distribution of language-modulated visual features closely matches that of the text description, as shown in Fig. 3(g). This is similar to standard object detection’s one-hot label prediction, but instead of being limited by the number of categories, we predict the position of text that is similar to objects.

The text distribution of the main object is constructed by element-wise summing the position labels of the associated decoupled text components:

$$P_{main} = \lambda_1 L_{main} + \lambda_2 L_{attri} + \lambda_3 L_{pron} + \lambda_4 L_{rel}, \quad (1)$$

where λ is the weight of different parts. $P_{auxi} = L_{auxi}$ represents the text distribution of the auxiliary object. The remaining objects’ text distribution is P_{oth} , with the final bit set to 1 (see \emptyset in Fig. 3(g)). Therefore, the text distribution of all candidate objects is $P_{text} = \{P_{main}, P_{auxi}, P_{oth}\} \in \mathbb{R}^{k \times l}$. The visual distribution of objects is produced by applying softmax to the output L_{pred} of the prediction head:

$$P_{obj} = \text{Softmax}(L_{pred}). \quad (2)$$

Their KL divergence is defined as the position-aligned loss:

$$\mathcal{L}_{pos} = \sum_{i=1}^k [P_{text}^i \log(P_{text}^i) - P_{text}^i \log(P_{obj}^i)]. \quad (3)$$

We highlight that “dense alignment” indicates that the target object is aligned with the positions of multiple components (Eq. (1)), significantly different from Beauty-DETR (and MDETR (Kamath et al. 2021) for 2D tasks), which only sparsely aligns with the object name’s position L_{main} .

2) Dense Semantic Aligned Loss Semantic alignment aims to learn the similarity of visual-text multimodal features through contrastive learning. The loss of semantic alignment is therefore defined as follows:

$$\mathcal{L}_{sem} = \sum_{i=1}^k \frac{1}{|\mathbf{T}_i^+|} \sum_{\mathbf{t}_i \in \mathbf{T}_i^+} -\log \left(\frac{\exp(w_+ * (\mathbf{o}_i^\top \mathbf{t}_i / \tau))}{\sum_{j=1}^l \exp(w_- * (\mathbf{o}_i^\top \mathbf{t}_j / \tau))} \right), \quad (4)$$

where \mathbf{o} and \mathbf{t} are the object and text features after linear projection, and $\mathbf{o}^\top \mathbf{t} / \tau$ is their similarity. \mathbf{t}_i is the positive text feature of the i_{th} candidate object, as shown in Fig. 3 (h). Taking the main object as an example, the positive text feature corresponding to it is:

$$\mathbf{t}_i \in \mathbf{T}_i^+ = \{\mathbf{t}_{main}, \mathbf{t}_{attri}, \mathbf{t}_{pron}, \mathbf{t}_{rel}\}, \quad (5)$$

and w_+ is the weight of each positive term. \mathbf{t}_j is the feature of all texts, but note that the similarity weight w_- for auxiliary object term \mathbf{t}_{auxi} is 2, while the rest weight 1.

Similarly, the semantic alignment of multiple text components (Eq. (5)) with visual features also illustrates our insight of “dense.” This is intuitive, such as “It is a brown chair with legs under a blackboard,” where the main object’s visual features should be not only similar to “chair” but also similar to “brown, legs” and distinct to “blackboard” as possible.

3.4 Task-Oriented Explicit Prediction

As a result of decoupling and dense alignment operations, object features have fused several types of textual semantic features, which can explicitly combine textual components to enable multiple visual-linguistic tasks. **1)** For the regular VG task of predicting the main object, we compute the similarity $S_{all} \in \mathbb{R}^k$ between the visual features of the candidate objects and the text features of the relevant components and then select the candidate with the highest score:

$$S_{all} = S_{main} + S_{attri} + S_{pron} + S_{rel} - S_{auxi}, \quad (6)$$

where $S_{main} = \text{Softmax}(\mathbf{o}^\top \mathbf{t}_{main} / \tau)$ denotes the similarity between the object feature and the main object component text feature, and other terms are also similar. **2)** It is also possible to identify related objects using part-text features. For instance, only use the attribute text component feature, and the similarity score is $S_{all} = S_{attri}$. **3)** For another challenging scenario, locating the auxiliary object mentioned in the description, similarly, we solely compute the similarity scores between the object features and the auxiliary component’s text features: $S_{all} = S_{auxi}$. Being able to infer the object based on the part of the text is a significant sign that the network has learned well-aligned and fine-grained visual-text feature space.

4 Experiments

4.1 Regular 3D Visual Grounding

1) Experiment settings We keep the same settings as existing works, with ScanRefer (Chen, Chang, and Nießner 2020) and SR3D/NR3D (Achlioptas et al. 2020) as datasets and IoU@0.25 and IoU@0.5 as metrics. Based on the visual data of ScanNet (Dai et al. 2017), an indoor 3D dataset, **ScanRefer** adds 51,583 manually annotated text descriptions about objects. These complex and free-form descriptions involve object categories and attributes such as colour, shape, size, and spatial position relationships. **SR3D/NR3D** is also proposed based on ScanNet, with SR3D including 83,572 simple machine-generated descriptions and NR3D containing 41,503 descriptions similar to ScanRefer’s human annotation. The *difference* is that in the ScanRefer configuration, detecting and locating objects is required, while SR3D/NR3D is simpler. It supplies additional GT boxes for all candidate objects and only needs to classify boxes and locate the target object.

2) Regular 3D visual grounding results **ScanRefer.** Table 1 reports the results on the ScanRefer dataset. **i)** Our method achieves state-of-the-art performance on all metrics by a substantial margin, with an overall improvement of 4.2% and 3.7% to 54.59% and 42.26% (the first time over 40% on metric IoU@0.5). **ii)** Previous studies proved that supplemented 2D images with detailed and dense semantics could learn better point cloud features. Surprisingly, we only use sparse 3D point cloud features and even outperformed 2D assistance methods. This illustrates that our decoupling and dense alignment strategies mine more efficient and meaningful visual-text co-representations. **iii)** Another finding is that the accuracy of most existing techniques is

less than 40% and 30% in the “multiple” setting because multiple means that the category of target objects mentioned in the language is not unique, with more interference candidates in the scene. However, we reached a remarkable 49.13% and 37.64%. We believe that in this complex setting, a finer-grained understanding of the text is required to identify similar objects. **iv)** The last row in Table 1 shows our method’s single-stage implementation without the object detection step (\mathcal{B} in Fig. 3) in both training and inference, illustrating that our approach can achieve SOTA performance without requiring an additional 3D object detector. **v)** The qualitative results are depicted in Fig. 4(a-c), which reveals that our method with an excellent perception of appearance attributes, spatial relationships, and even ordinal numbers.

SR3D/NR3D. Table 2 shows the accuracy on the SR3D/NR3D dataset, where we achieve the best performance of 67.8% and 51.5%. In SR3D, the language descriptions are concise, and the object is easy to identify, leaving limited room for improvement. In NR3D, descriptions are too detailed, posing additional challenges for text decoupling and resulting in a performance marginally lower than 54.6% of ScanRefer.

3) Ablation studies **Baseline.** 3D-SPS (3D version) is the SOTA of **implicit** techniques. We denote it as **A** in Table 3. Beauty-DETR is a representative of explicit fashion, but it only sparsely considers the words of the object’s name in the text. We denote it as **B** in Table 3, a **sparse explicit** method.

Analysis. **i)** (a) is our implementation of the sparse explicit idea, using only the “Main object” component decoupled from text, which achieves better performance than **B**, verifying the accuracy of our text decoupling. **ii)** Explicit methods (**B** and (a)) are significantly superior to the implicit method (**A**) because we explicitly select the text features most relevant to the target object to minimize ambiguity, while self-attention guarantees that global text information is not lost. **iii)** Dense aligned methods ((b)-(h)) outperform sparse alignments (**B** and (a)) since more fine-grained visual-linguistic feature fusion is produced. **iv)** (b)-(e) indicate that adding any other component to the “Main object” can improve performance, demonstrating the validity of each text component. The component of “Attribute” aid in identifying features such as color, shape, etc., frequently mentioned in text descriptions. Unexpectedly, “Pronoun” components such as “it, that, and which” have little meaning when used alone but also function in our method, indicating that the pronoun learned contextual information from the sentence. Understanding the spatial relationships between objects is facilitated by the “Relationship” component. The component “Auxiliary object” serves as a negative term in the loss (Eq. (4)). During inference (Eq. (6)), its similarity is subtracted in the hopes that the predicted object is as dissimilar to it as possible. **v)** (f)-(h) combine different components to make performance gains and reach the peak when all are involved, indicating that the functions of each component can be complementary, and there may be no overlap between the features of each one. The result demonstrates that our method effectively decouples and matches multimodal features.

Method	Reference	Modality	Unique (~19%)		Multiple (~81%)		Overall	
			0.25	0.5	0.25	0.5	0.25	0.5
ScanRefer	(Chen, Chang, and Nießner 2020)	3D	67.64	46.19	32.06	21.26	38.97	26.10
		3D+2D	76.33	53.51	32.73	21.11	41.19	27.40
ReferIt3D	(Achlioptas et al. 2020)	3D	53.8	37.5	21.0	12.8	26.4	16.9
TGNN	(Huang et al. 2021)	3D	68.61	56.80	29.84	23.18	37.37	29.70
InstanceRefer	(Yuan et al. 2021)	3D	77.45	66.83	31.27	24.77	40.23	32.93
SAT	(Yang et al. 2021)	3D+2D	73.21	50.83	37.64	25.16	44.54	30.14
FFL-3DOG	(Feng et al. 2021)	3D	78.80	67.94	35.19	25.70	41.33	34.01
3DVG-Transformer	(Zhao et al. 2021)	3D	77.16	58.47	38.38	28.70	45.90	34.47
		3D+2D	81.93	60.64	39.30	28.42	47.57	34.67
3D-SPS	(Luo et al. 2022)	3D	81.63	64.77	39.48	29.61	47.65	36.43
		3D+2D	84.12	66.72	40.32	29.82	48.82	36.98
3DJCG	(Cai et al. 2022)	3D	78.75	61.30	40.13	30.08	47.62	36.14
		3D+2D	83.47	64.34	41.39	30.82	49.56	37.33
Beauty-DETR †	(Jain et al. 2022)	3D	82.88	64.98	44.73	33.97	50.42	38.60
EDA	-	3D	85.76	68.57	49.13	37.64	54.59 (+4.2%)	42.26 (+3.7%)
EDA (single-stage) §	-	3D	86.40	69.42	48.11	36.82	53.83	41.70

Table 1: The 3D visual grounding results on ScanRefer, accuracy evaluated by IoU 0.25 and IoU 0.5. † The accuracy in the table is reevaluated using our parsed text labels because the performance reported by Beauty-DETR used GT text labels and ignored some challenging samples (see supplementary materials for more details). § The pure single-stage implementation without the assistance of the additional 3D object detection step (dotted arrows in Fig. 3).

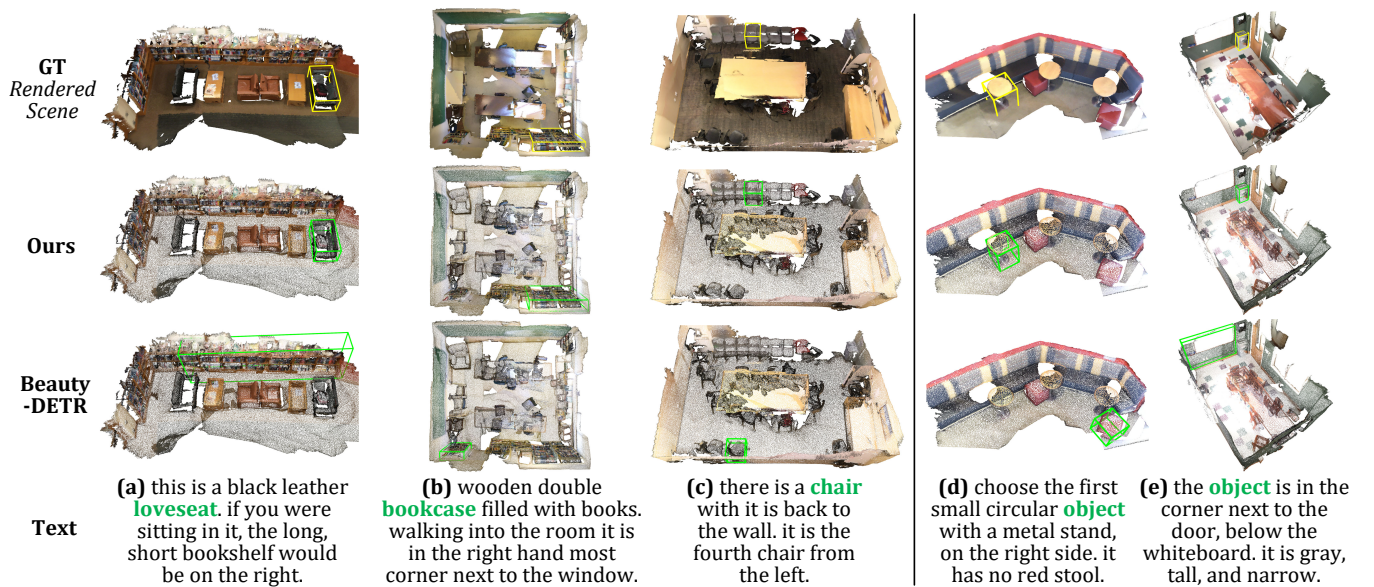


Figure 4: Qualitative results with ScanRefer texts. (a-c): Regular 3D visual grounding. (d-e): Grounding without object name.

4.2 Grounding without Object Name (VG-w/o-ON)

1) Experiment settings To avoid the model learning inductive biases about object categories while ignoring other attributes, we propose a new task: grounding objects without object names. Specifically, we manually replace the category of the target object with “object” in the ScanRefer validation set. For instance: “this is a brown wooden chair” becomes “this is a brown wooden object”. A total of 9253 samples were annotated, and another 255 ambiguous samples were discarded. Without retraining, we perform comparative ex-

periments using our best model and comparison approaches’ best models that were pre-trained for regular VG.

2) Result and analysis Table 4 reports the experimental results. **i)** The performance of all methods on this challenging task is significantly lower than that of regular VG (see Table. 1), indicating that object categories provide rich semantic information, which is also conducive to classifying features. It’s accessible to produce the category’s inductive bias, especially in the “unique” setting. **ii)** The explicit sparse alignment strategy represented by Beauty-DETR per-

Method	SR3D	NR3D
ReferIt3D (Achlioptas et al. 2020)	39.8	35.6
TGNN (Huang et al. 2021)	45	37.3
TransRefer3D (He et al. 2021)	57.4	42.1
InstanceRefer (Yuan et al. 2021)	48	38.8
3DVG-Transformer (Zhao et al. 2021)	51.4	40.8
FFL-3DOG (Feng et al. 2021)	-	41.7
SAT (Yang et al. 2021)	57.9	49.2
3DReferTrans. (Abdelreheem et al. 2022)	47	39
LanguageRefer (Roh et al. 2022)	56	43.9
Beauty-DETR †(Jain et al. 2022)	65.6	49.1
EDA (Ours)	67.8	51.5

Table 2: Performance on SR3D/NR3D datasets. † Reevaluated by parsed text labels.

Method		Main	Attri.	Pron.	Auxi.	Rel.	@0.25	@0.5	
Implicit	A						47.7	36.4	
	B	✓					50.4	38.6	
Explicit	Spa.	(a)	✓				52.1	40.5	
		(b)	✓	✓			53.1	41.3	
	Dense	(c)	✓		✓		52.9	40.8	
		(d)	✓			✓	52.9	41.0	
		(e)	✓				✓	52.8	40.7
		(f)	✓	✓	✓			53.8	41.8
		(g)	✓	✓	✓	✓		54.2	42.3
		(h)	✓	✓	✓	✓	✓	54.6	42.3

Table 3: Ablation studies of different text components on the ScanRefer validation set.

forms comparably to implicit methods, or even worse. We analyse that in the Transformer architecture, a word’s feature includes both the word meaning and the entire sentence meaning. However, when the word “object” is devoid of information, its feature degenerates into the global sentence feature, comparable to implicit strategy. Therefore, sparse alignment alone is insufficient. **iii)** Our method achieves absolute lead with the performance of 26.5% and 21.2%, which is over 10% higher than other methods. This demonstrates that our proposed text decoupling and dense alignment enable fine-grained visual-linguistic feature matching, where the model identifies the visual features most similar to other text components (*e.g.* attributes, relations, etc.). **iv)** Fig. 4(d-e) shows qualitative examples. Even without knowing the target’s name, our method can infer it by other cues, while Beauty-DETR’s performance drops catastrophically.

Table 5 shows the performance of grounding objects using a single decoupled text component. Such as, “Attri.” means that the visual features only calculate the similarity with the attribute component feature, $S_{all} = S_{attri}$ in Eq. (6). In Beauty-DETR, the “Attri.” component outperforms the “Main” and “Pron.” components, which is evident because, in this setting, attribute words contain richer cues. However, in our method, the three components achieve similar performance. Therefore, as indicated in the last column of Table 5, we statistically analyze the probability that the three text component features match the same object in the correctly predicted samples. Under the supervision of our dense

Method	VG-w/o-ON		VG-AO	
	@0.25	@0.5	@0.25	@0.5
ScanRefer	10.5	6.2	-	-
TGNN	12.0	9.7	-	-
InstanceRefer	13.9	11.5	-	-
Beauty-DETR	12.0	8.9	7.8	4.0
EDA (Ours)	26.5	21.2	58.1	48.3

Table 4: Performance of two new tasks on ScanRefer.

	Main	Attri.	Pron.	Prob.
Beauty-DETR	11.7	13.0	11.4	49.60%
EDA (Ours)	23.7	23.7	23.6	96.40%

Table 5: Performance of the single text component.

aligned losses, the text features of these three components are highly shared, allowing for a more comprehensive aggregation of target-related cues to localize objects.

4.3 Grounding Auxiliary Object (VG-AO)

1) Experiment settings To evaluate the model’s capacity to discriminate between multiple objects mentioned in language descriptions, we propose another new task: locating the auxiliary object. Since there is no ground truth for auxiliary objects in ScanRefer, we search all GT boxes for the box closest to the main object and whose category matches the auxiliary one to use as the pseudo-GT box for the auxiliary object. As the sub-validation set for this task, 5906 samples with auxiliary object descriptions are selected from the ScanRefer validation set.

2) Result and analysis Using the proposed text decoupling method, we obtain text features and locate the auxiliary object based on $S_{all} = S_{auxi}$ in Eq. (6), as shown in Table 4. During training on the ScanRefer dataset, Beauty-DETR only aligns the visual and textual features of the “main object”, making it nearly hard to find auxiliary objects. We additionally supervised auxiliary objects during training and achieved comparable performance of 58.1% and 48.3% to the main object localization. Other works are not compared since their coupled nature makes it cannot identify auxiliary object features. The results demonstrate that it is required to decouple text and supervise the alignment of individual text components with vision.

5 Conclusion

This paper introduces a new 3D visual-language learning strategy that enables fine-grained visual-language fusion by decoupling text and being supervised by dense aligned loss. In addition, two challenging new tasks are presented to evaluate the model’s capacity. Extensive quantitative and qualitative analyses demonstrate its superior performance. Essentially, it is not confined to the feature extraction backbone and can be easily extended and applied to other cross-modal tasks. However, its limitation is that text decoupling may fail in the case of lengthy descriptions, resulting in a performance decrease.

Supplementary Material

Section A of the supplementary material provides the implementation details of the individual modules and the network training details. In Section B, we supplement with additional experiments and quantitative analyses. Finally, in Section C, we present visualization results and qualitative analysis.

A Implementation details

Text decoupling module. The maximum length of the text is $l=256$, and the absence bit of the position label $L \in \mathbb{R}^{1 \times l}$ is padded with 0. Not every sentence can be decoupled into five semantic components, but the most fundamental “main object” is required. In some cases, such as grammatical errors, or word typos, resulting in no components being decoupled, we add the prompt “this is an object.” at the beginning of the sentence so that the word “object” becomes the main component.

Encoder-Decoder. We keep hyperparameters consistent with Beauty-DETR. The point cloud is tokenized as $\mathcal{V} \in \mathbb{R}^{n \times d}$ by the pointnet++ pre-trained on ScanNet. The text is tokenized as $\mathcal{T} \in \mathbb{R}^{l \times d}$ by the pre-trained d RoBERTa. Following object detection, the position and category of the boxes are embedded separately and concatenated as the box token $\mathcal{B} \in \mathbb{R}^{b \times d}$. The encoder, for visual-text feature extraction and modulation, is $N_E=3$ layers. The decoder with $N_E=6$ layers generates candidate object features $\mathcal{Q} \in \mathbb{R}^{k \times d}$. Where $n=1024$ denotes the number of seed points, $l=256$ the number of texts, $b=132$ the number of detection boxes, $k=256$ the number of candidate objects, and $d=288$ the feature dimension.

Losses. 1) In the position alignment loss \mathcal{L}_{pos} , the weights of each component in the Eq.(1) used to construct the text distribution of the main object are as follows: $\lambda_1=0.6$, $\lambda_2=\lambda_3=0.2$, $\lambda_4=0.1$. This indicates that the weight of the “main object” component L_{main} is higher, which is obvious. The “relational” component L_{rel} with lower weight because it affects both the main and auxiliary objects. **2)** In the semantic alignment loss \mathcal{L}_{sem} , the weight w_+ follows a similar trend. The four features $t_{main}, t_{attri}, t_{pron}, t_{rel}$ are weighted by 1.0, 0.2, 0.2, and 0.1, respectively. The weight w_- acts on the negative item, where the feature weight of the auxiliary object is 2 and the remainder weighs 1. The purpose is to differentiate the features of the main object from the auxiliary objects. In the body text, Eq.(4) represents the loss for all candidate objects \mathcal{L}_{sem_o} , whereas the loss for text \mathcal{L}_{sem_t} is omitted due to limited space, and its definition is similar:

$$\mathcal{L}_{sem.t} = \sum_{i=1}^l \frac{w_+}{|\mathbf{O}_i^+|} \sum_{\mathbf{o}_i \in \mathbf{O}_i^+} -\log \left(\frac{\exp(\mathbf{t}_i^\top \mathbf{o}_i / \tau)}{\sum_{j=1}^k \exp(\mathbf{t}_i^\top \mathbf{o}_j / \tau)} \right), \quad (7)$$

where \mathbf{O}_i denotes the object aligned with the i_{th} word, and w_+ equates the weight in Eq.(4). In the code implementation, the semantic alignment loss is the mean of the two:

$$\mathcal{L}_{sem} = (\mathcal{L}_{sem_o} + \mathcal{L}_{sem_t}) / 2. \quad (8)$$

3) We optimize the model with the following total loss:

$$\mathcal{L} = 0.5\mathcal{L}_{pos} + 0.5\mathcal{L}_{sem} + 5\mathcal{L}_{box} + \mathcal{L}_{iou}, \quad (9)$$

where \mathcal{L}_{box} is the L1 regression loss of the object’s position and size, and \mathcal{L}_{iou} is the object’s 3D IoU loss.

Training details. The code is implemented based on PyTorch. We set the batch size to 12 on four 24-GB NVIDIA-RTX-3090 GPUs. For ScanRefer, we use a $2e-3$ learning rate for the visual encoder and a $2e-4$ learning rate for all other layers. It takes about 15 minutes per epoch, and around epoch 60, the best model appears. The learning rates for SR3D are $1e-3$ and $1e-4$, 25 minutes per epoch, requiring around 40 epochs of training. The learning rates for NR3D are set at $5e-4$ and $5e-5$, 15 minutes per epoch, and around 160 epochs are trained. Since SR3D is composed of 83572 brief machine-generated sentences, convergence is easier. ScanRefer and NR3D are comprised of 51583 and 41503 human-annotated free-form complex descriptions, respectively, and require more training time.

B Additional experiments

B.1 Regular 3D Visual Grounding

1) The explanation of the Beauty-DETR’s performance. Given a sentence, such as “*It is a brown chair with armrests and four legs. It is directly under a blackboard*”, our text decoupling module determines that “chair” is the main object based on grammatical analysis and thus obtains the position label $L_{main} = 0000100\dots$. However, in the official implementation of Beauty-DETR, which requires an additional ground truth class for the target object, its input is: “*<object name> chair. <Description> It is a brown chair ...*”. Then search for the position where the object name “chair” appears in the sentence as a position label.

This presents some problems: **i)** It is unfair to use GT labels during inference; **ii)** Descriptions may employ synonyms for the category “chair,” such as “armchair, office-chair, and loveseat,” leading to a failed search position label. **iii)** Sometimes, the object name is not mentioned, such as when it is replaced by the word “object.” In the NR3D validation set, Beauty-DETR removed 800 such challenging samples, which is about 5%. To be fair, we re-evaluate it using the position labels obtained by the proposed text decoupling module, as displayed in the second row in Tab. 6.

	ScanRefer		SR3D	NR3D
	IoU0.25	IoU0.5		
Official	52.2	39.8	67.1	55.4
Re-evaluation	50.4	38.6	65.6	49.1

Table 6: Performance of Beauty-DETR.

2) Evaluation of ScanRefer using GT box. In the ScanRefer dataset, only the point cloud is provided as visual input, requiring object detection and language-based object

grounding. Conversely, SR3D/NR3D offers additional GT boxes of candidate objects. Therefore, we further evaluate the ScanRefer dataset by GT boxes. As shown in Tab. 7, our performance improves significantly without retraining, particularly in the unique setting where accuracy exceeds 90%. This demonstrates that more accurate object detection can further enhance our performance.

Method	Unique		Multiple		Overall	
	0.25	0.5	0.25	0.5	0.25	0.5
Beauty-DETR	85.62	68.64	46.07	35.51	52.0	40.5
EDA (Ours)	90.91	75.33	51.71	40.66	57.6	45.8

Table 7: Performance on ScanRefer using GT box.

B.2 Grounding without Object Name (VG-w/o-ON)

We perform ablation studies on individual components in the new task of grounding without mentioning the object name. Tab.8 illustrates a tendency consistent with ablation analysis in the standard VG task: each component contributes, and the best performance is reached when all parts participate.

	Main	Attri.	Pron.	Auxi.	Rel.	IoU0.25	IoU0.5
(a)	✓					21.8	17.1
(b)	✓	✓				23.2	17.8
(c)	✓		✓			23.7	18.6
(d)	✓			✓		23.2	18.4
(e)	✓				✓	25.7	19.6
(f)	✓	✓	✓			24.2	18.5
(g)	✓	✓	✓	✓		24.0	18.8
(h)	✓	✓	✓	✓	✓	26.5	21.2

Table 8: Ablation studies on the VG-w/o-ON task.

Importantly, we find that the gain of all the additional components is higher than that of the regular VG task, which is consistent with our insight. This is because the model requires more consideration of other clues to locate the object in the challenging task without the object’s name. Moreover, the relational component provides the most benefit, as the spatial relationship between the main and auxiliary objects is particularly advantageous in this case.

B.3 Grounding Auxiliary Object (VG-AO)

Tab.4 in the body text shows the performance of auxiliary object localization on the ScanRefer dataset, where Beauty-DETR does not account for the loss of auxiliary objects, resulting in a significant performance decrease. In the SR3D dataset, EDA and Beauty-DETR supervise both the main and auxiliary objects, as seen in Tab.9. Due to the brief description of the SR3D and the ease of object localization, there are no notable performance differences between the two methods. This demonstrates that only supervising the main object is insufficient for locating auxiliary objects. It is preferable to align multiple objects mentioned in a sentence, and text decoupling is required to do this.

	main object	auxiliary object
Beauty-DETR	65.6	73.8
EDA (Ours)	67.8	73.6

Table 9: The main object and auxiliary object localization performance on SR3D dataset.

B.4 Language Modulated 3D Object Detection

We maintain the same experimental setup as Beauty-DETR to evaluate the performance of 3D object detection on ScanNet. The 18 classes in ScanNet are concatenation into a sentence: “*bed. bookshelf. cabinet. chair. counter. curtain. desk. door ...*” as text input. Output the bounding boxes and classes of all objects in the point cloud. As shown in Tab. 10, our model after text modulation on the ScanRefer achieves 1.1% and 1.5% higher performance than Beauty-DETR, to 64.1% and 45.3%. This demonstrates the potential of our method in other 3D vision and language cross-modality tasks.

Method	mAP@0.25	mAP@0.5
DETR+KPS+iter †	59.9	-
3DETR with PointNet++ †	61.7	-
Beauty-DETR trained on ScanRefer	63.0	43.8
EDA trained on ScanRefer (Ours)	64.1	45.3

Table 10: 3D Object detection performance on ScanNet. † The accuracy is provided by Beauty-DETR.

C Qualitative analysis

1) Regular 3D Visual Grounding. Qualitative results on the regular 3D visual grounding task are displayed in Fig. 6, 7, 8. **i)** Fig. 6 indicates that compared to Beauty-DETR, our method has a superior perception of appearance, enabling the identification of objects based on their attributes among several candidates of the same class. This improvement is made possible by the alignment of our decoupled text attribute component with visual features. **ii)** Fig. 7 demonstrates that our method exhibits excellent spatial awareness, such as orientation and position relationships between objects. The alignment of our decoupled relational component with visual features and the positional encoding of Transformer may be advantageous to this capability. **iii)** Furthermore, we surprisingly found that our method also has a solid understanding of ordinal numbers, as shown in Fig. 8, probably because we parsed ordinal numbers as part of the attribute component of the object. These examples demonstrate that text decoupling and dense alignment enable fine-grained visual-linguistic matching.

2) Grounding without Object Name (VG-w/o-ON). The visualization results of this challenging task are shown in Fig. 5. Since the target object’s name is not provided, the model must make inferences based on appearance attributes and positional relationships with auxiliary objects. However, other contrastive methods perform weakly on this task because they rely heavily on object names to exclude interference candidates, weakening the learning of other attributes.



Figure 5: 3D visual grounding without mentioning the object name, where the word “object” replaces the target’s name.

3) Grounding Auxiliary Object (VG-AO). Fig. 9 presents the results of simultaneous localize the main and auxiliary objects by EDA, shown in green and red, respectively. Text decoupling enables the model to comprehend multiple objects referenced in the description, and dense alignment assigns visual features to each object, which is impossible with coupled paradigm techniques.

4) Failure Case Analysis. Although our method delivers state-of-the-art performance, there are still a significant number of failure occurrences, which we analyze visually. **i)** Many language descriptions are intrinsically ambiguous, as illustrated in Fig. 10(a-c), especially in the “multiple” setting, the appearance attributes and spatial relationships of the target object are not unique, and there are multiple alternatives for candidate objects that match the requirements. **ii)** The text parsing error may occur owing to the language description’s complexity and diversity. Such as, the GT object in Fig. 10(d) is a desk, but we parse it as a window; the GT object in Fig. 10(e) is a box, but we parse it as a piano. **iii)**

There are also some cases where cross-modal feature matching fails even though the text parses well.

We suggest that future efforts can focus on **i)** accurate text parsing for complicated and diversified descriptions; **ii)** more efficient and fine-grained cross-modal feature fusion; **iii)** alleviating the data scarcity problem in 3D vision-language learning.

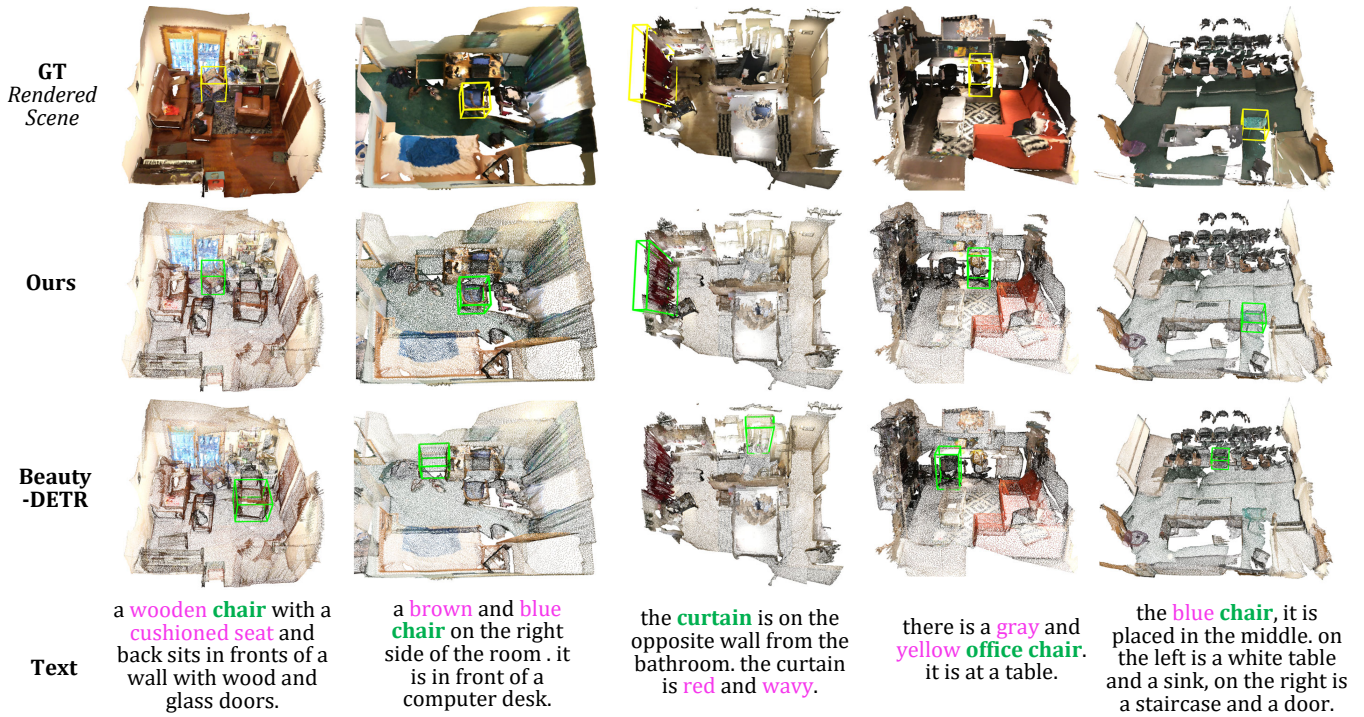


Figure 6: Qualitative comparison of the regular 3D VG task. Our method has a superior perception of appearance attributes.



Figure 7: Qualitative comparison of the regular 3D VG task. Our method has a superior perception of spatial relationships.

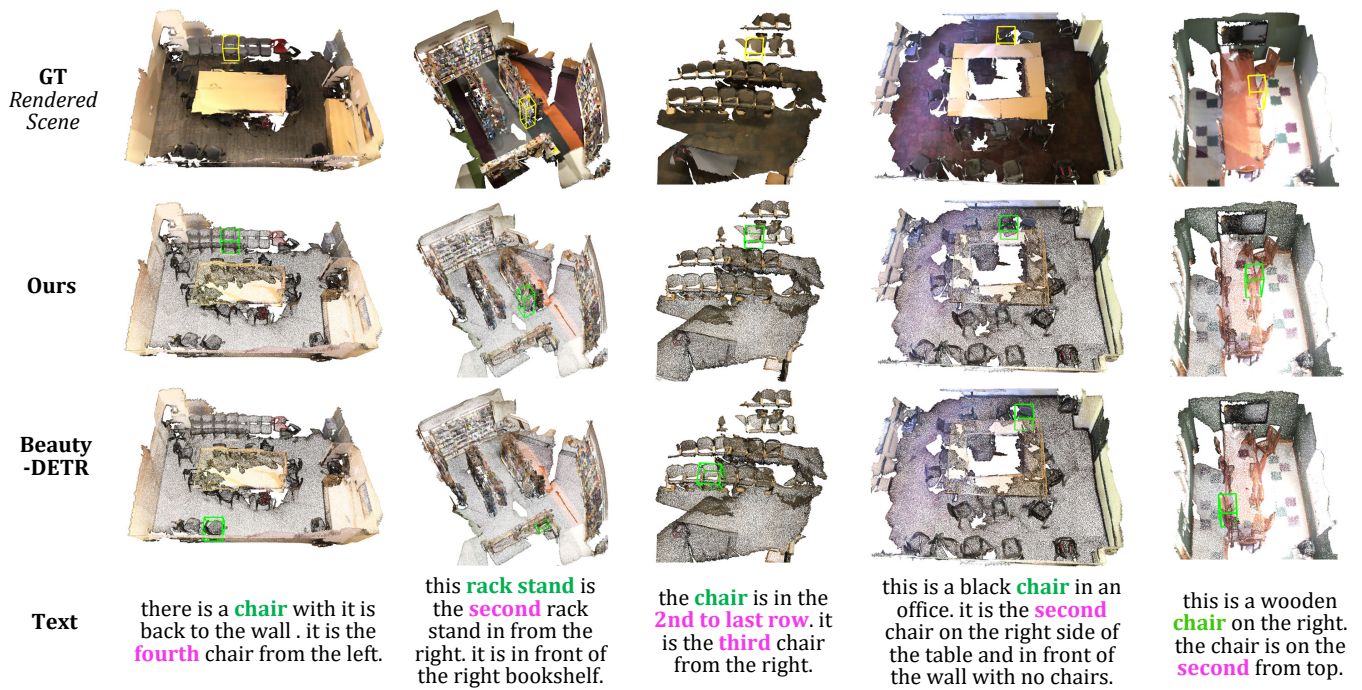


Figure 8: Qualitative comparison of the regular 3D VG task. Challenging cases with ordinal numbers.

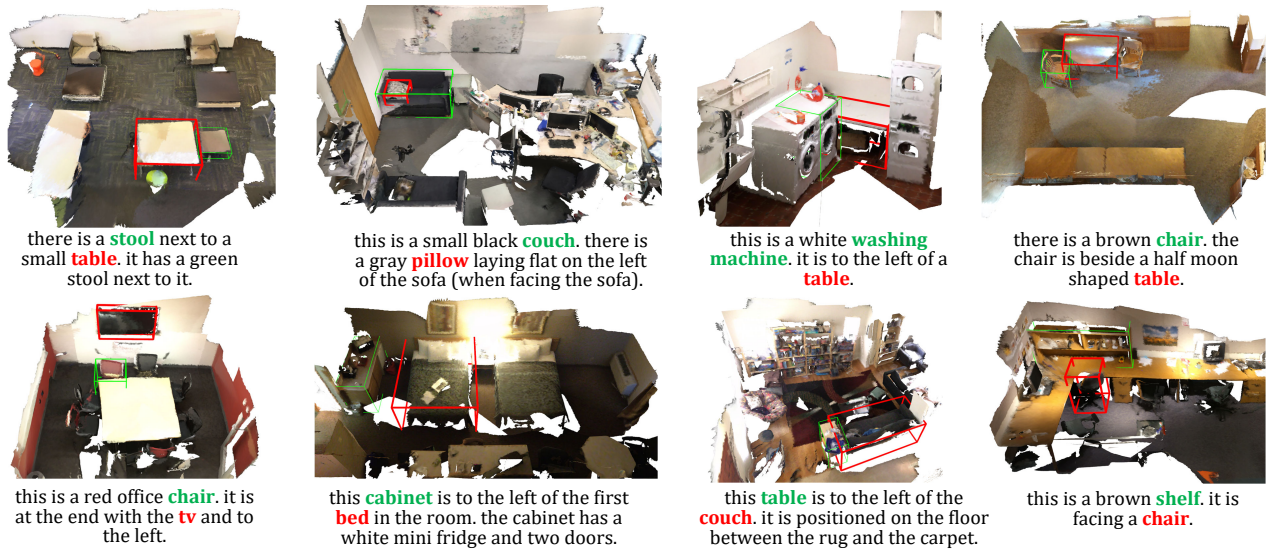


Figure 9: Simultaneously grounding the main and auxiliary objects, shown in green and red, respectively.

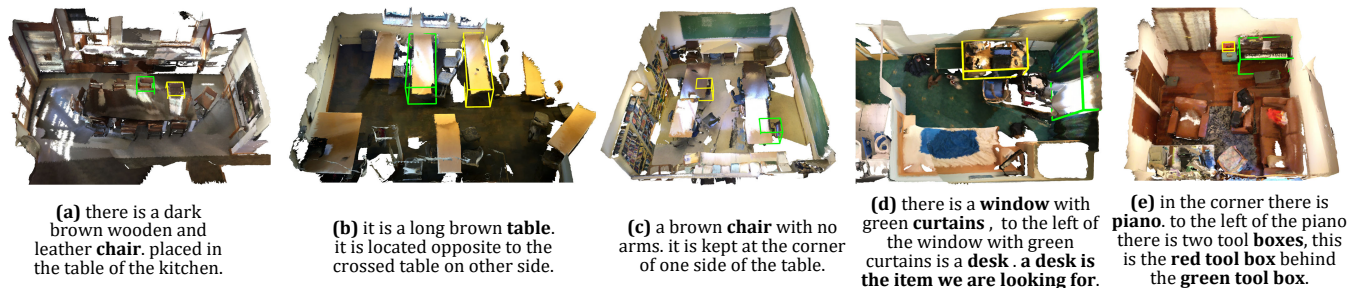


Figure 10: Failure cases, with the GT box and prediction box shown in yellow and green, respectively.

References

- Abdelreheem, A.; Upadhyay, U.; Skorokhodov, I.; Al Yahya, R.; Chen, J.; and Elhoseiny, M. 2022. 3DRefTransformer: Fine-Grained Object Identification in Real-World Scenes Using Natural Language. In *Proceedings of the IEEE/CVF Winter Conference on Applications of Computer Vision*, 3941–3950. 2, 7
- Achlioptas, P.; Abdelreheem, A.; Xia, F.; Elhoseiny, M.; and Guibas, L. 2020. Referit3d: Neural listeners for fine-grained 3d object identification in real-world scenes. In *European Conference on Computer Vision*, 422–440. Springer. 1, 2, 5, 6, 7
- Cai, D.; Zhao, L.; Zhang, J.; Sheng, L.; and Xu, D. 2022. 3DJCG: A Unified Framework for Joint Dense Captioning and Visual Grounding on 3D Point Clouds. In *Proceedings of the IEEE/CVF Conference on Computer Vision and Pattern Recognition*, 16464–16473. 2, 3, 6
- Chen, D. Z.; Chang, A. X.; and Nießner, M. 2020. Scanrefer: 3d object localization in rgb-d scans using natural language. In *European Conference on Computer Vision*, 202–221. Springer. 1, 5, 6
- Chen, D. Z.; Wu, Q.; Nießner, M.; and Chang, A. X. 2021a. D3Net: A Speaker-Listener Architecture for Semi-supervised Dense Captioning and Visual Grounding in RGB-D Scans. *arXiv preprint arXiv:2112.01551*. 2
- Chen, Z.; Gholami, A.; Nießner, M.; and Chang, A. X. 2021b. Scan2cap: Context-aware dense captioning in rgb-d scans. In *Proceedings of the IEEE/CVF Conference on Computer Vision and Pattern Recognition*, 3193–3203. 2
- Dai, A.; Chang, A. X.; Savva, M.; Halber, M.; Funkhouser, T.; and Nießner, M. 2017. Scannet: Richly-annotated 3d reconstructions of indoor scenes. In *Proceedings of the IEEE conference on computer vision and pattern recognition*, 5828–5839. 5
- Devlin, J.; Chang, M.-W.; Lee, K.; and Toutanova, K. 2018. Bert: Pre-training of deep bidirectional transformers for language understanding. *arXiv preprint arXiv:1810.04805*. 2
- Dosovitskiy, A.; Beyer, L.; Kolesnikov, A.; Weissenborn, D.; Zhai, X.; Unterthiner, T.; Dehghani, M.; Minderer, M.; Heigold, G.; Gelly, S.; Uszkoreit, J.; and Hounsford, N. 2021. An Image is Worth 16x16 Words: Transformers for Image Recognition at Scale. In *International Conference on Learning Representations*. 2
- Feng, M.; Li, Z.; Li, Q.; Zhang, L.; Zhang, X.; Zhu, G.; Zhang, H.; Wang, Y.; and Mian, A. 2021. Free-form description guided 3d visual graph network for object grounding in point cloud. In *Proceedings of the IEEE/CVF International Conference on Computer Vision*, 3722–3731. 2, 6, 7
- He, D.; Zhao, Y.; Luo, J.; Hui, T.; Huang, S.; Zhang, A.; and Liu, S. 2021. TransRefer3D: Entity-and-Relation Aware Transformer for Fine-Grained 3D Visual Grounding. In *Proceedings of the 29th ACM International Conference on Multimedia*, 2344–2352. 2, 7
- He, K.; Fan, H.; Wu, Y.; Xie, S.; and Girshick, R. 2020. Momentum contrast for unsupervised visual representation learning. In *Proceedings of the IEEE/CVF conference on computer vision and pattern recognition*, 9729–9738. 2
- Huang, P.-H.; Lee, H.-H.; Chen, H.-T.; and Liu, T.-L. 2021. Text-guided graph neural networks for referring 3d instance segmentation. In *Proceedings of the AAAI Conference on Artificial Intelligence*, volume 35, 1610–1618. 2, 6, 7
- Jain, A.; Gkanatsios, N.; Mediratta, I.; and Fragkiadaki, K. 2022. Looking Outside the Box to Ground Language in 3D Scenes. In *European Conference on Computer Vision*. Springer. 2, 3, 6, 7
- Jiang, L.; Zhao, H.; Shi, S.; Liu, S.; Fu, C.-W.; and Jia, J. 2020. Pointgroup: Dual-set point grouping for 3d instance segmentation. In *Proceedings of the IEEE/CVF conference on computer vision and pattern recognition*, 4867–4876. 2
- Jiao, Y.; Chen, S.; Jie, Z.; Chen, J.; Ma, L.; and Jiang, Y.-G. 2022. MORE: Multi-Order RELation Mining for Dense Captioning in 3D Scenes. *arXiv preprint arXiv:2203.05203*. 2
- Kamath, A.; Singh, M.; LeCun, Y.; Synnaeve, G.; Misra, I.; and Carion, N. 2021. MDETR-modulated detection for end-to-end multi-modal understanding. In *Proceedings of the IEEE/CVF International Conference on Computer Vision*, 1780–1790. 4
- Kumar, S.; Patro, B. N.; and Namboodiri, V. P. 2022. Auto QA: The Question Is Not Only What, but Also Where. In *Proceedings of the IEEE/CVF Winter Conference on Applications of Computer Vision*, 272–281. 2
- Liu, H.; Lin, A.; Han, X.; Yang, L.; Yu, Y.; and Cui, S. 2021a. Refer-it-in-rgbd: A bottom-up approach for 3d visual grounding in rgbd images. In *Proceedings of the IEEE/CVF Conference on Computer Vision and Pattern Recognition*, 6032–6041. 3
- Liu, Y.; Ott, M.; Goyal, N.; Du, J.; Joshi, M.; Chen, D.; Levy, O.; Lewis, M.; Zettlemoyer, L.; and Stoyanov, V. 2019. Roberta: A robustly optimized bert pretraining approach. *arXiv preprint arXiv:1907.11692*. 3
- Liu, Y.; Wan, B.; Zhu, X.; and He, X. 2020. Learning cross-modal context graph for visual grounding. In *Proceedings of the AAAI Conference on Artificial Intelligence*, volume 34, 11645–11652. 2
- Liu, Z.; Zhang, Z.; Cao, Y.; Hu, H.; and Tong, X. 2021b. Group-free 3d object detection via transformers. In *Proceedings of the IEEE/CVF International Conference on Computer Vision*, 2949–2958. 3
- Luo, J.; Fu, J.; Kong, X.; Gao, C.; Ren, H.; Shen, H.; Xia, H.; and Liu, S. 2022. 3D-SPS: Single-Stage 3D Visual Grounding via Referred Point Progressive Selection. In *Proceedings of the IEEE/CVF Conference on Computer Vision and Pattern Recognition*, 16454–16463. 2, 3, 6
- Qi, C. R.; Litany, O.; He, K.; and Guibas, L. J. 2019. Deep hough voting for 3d object detection in point clouds. In *proceedings of the IEEE/CVF International Conference on Computer Vision*, 9277–9286. 2
- Qi, C. R.; Yi, L.; Su, H.; and Guibas, L. J. 2017. Pointnet++: Deep hierarchical feature learning on point sets in a metric space. *Advances in neural information processing systems*, 30. 3

Qi, Y.; Wu, Q.; Anderson, P.; Wang, X.; Wang, W. Y.; Shen, C.; and Hengel, A. v. d. 2020. Reverie: Remote embodied visual referring expression in real indoor environments. In *Proceedings of the IEEE/CVF Conference on Computer Vision and Pattern Recognition*, 9982–9991. [2](#)

Radford, A.; Kim, J. W.; Hallacy, C.; Ramesh, A.; Goh, G.; Agarwal, S.; Sastry, G.; Askell, A.; Mishkin, P.; Clark, J.; et al. 2021. Learning transferable visual models from natural language supervision. In *International Conference on Machine Learning*, 8748–8763. PMLR. [2](#)

Ramesh, A.; Dhariwal, P.; Nichol, A.; Chu, C.; and Chen, M. 2022. Hierarchical text-conditional image generation with clip latents. *arXiv preprint arXiv:2204.06125*. [2](#)

Roh, J.; Desingh, K.; Farhadi, A.; and Fox, D. 2022. Langugerefer: Spatial-language model for 3d visual grounding. In *Conference on Robot Learning*, 1046–1056. PMLR. [7](#)

Rozenberszki, D.; Litany, O.; and Dai, A. 2022. Language-Grounded Indoor 3D Semantic Segmentation in the Wild. *arXiv preprint arXiv:2204.07761*. [2](#)

Schuster, S.; Krishna, R.; Chang, A.; Fei-Fei, L.; and Manning, C. D. 2015. Generating semantically precise scene graphs from textual descriptions for improved image retrieval. In *Proceedings of the fourth workshop on vision and language*, 70–80. [3](#)

Vaswani, A.; Shazeer, N.; Parmar, N.; Uszkoreit, J.; Jones, L.; Gomez, A. N.; Kaiser, Ł.; and Polosukhin, I. 2017. Attention is all you need. *Advances in neural information processing systems*, 30. [2](#)

Wang, H.; Zhang, C.; Yu, J.; and Cai, W. 2022. Spatiality-guided Transformer for 3D Dense Captioning on Point Clouds. *arXiv preprint arXiv:2204.10688*. [2](#)

Wu, H.; Mao, J.; Zhang, Y.; Jiang, Y.; Li, L.; Sun, W.; and Ma, W.-Y. 2019. Unified visual-semantic embeddings: Bridging vision and language with structured meaning representations. In *Proceedings of the IEEE/CVF Conference on Computer Vision and Pattern Recognition*, 6609–6618. [3](#)

Yang, Z.; Zhang, S.; Wang, L.; and Luo, J. 2021. Sat: 2d semantics assisted training for 3d visual grounding. In *Proceedings of the IEEE/CVF International Conference on Computer Vision*, 1856–1866. [2](#), [3](#), [6](#), [7](#)

Yuan, Z.; Yan, X.; Liao, Y.; Guo, Y.; Li, G.; Cui, S.; and Li, Z. 2022. X-trans2cap: Cross-modal knowledge transfer using transformer for 3d dense captioning. In *Proceedings of the IEEE/CVF Conference on Computer Vision and Pattern Recognition*, 8563–8573. [2](#)

Yuan, Z.; Yan, X.; Liao, Y.; Zhang, R.; Wang, S.; Li, Z.; and Cui, S. 2021. Instancerefer: Cooperative holistic understanding for visual grounding on point clouds through instance multi-level contextual referring. In *Proceedings of the IEEE/CVF International Conference on Computer Vision*, 1791–1800. [2](#), [6](#), [7](#)

Zhao, L.; Cai, D.; Sheng, L.; and Xu, D. 2021. 3DVG-Transformer: Relation modeling for visual grounding on point clouds. In *Proceedings of the IEEE/CVF International Conference on Computer Vision*, 2928–2937. [2](#), [6](#), [7](#)